# Monte Carlo lattice simulation of amphiphilic systems in two and three dimensions

R. G. Larson

Citation: The Journal of Chemical Physics **89**, 1642 (1988); doi: 10.1063/1.455110
View online: http://dx.doi.org/10.1063/1.455110
View Table of Contents: http://scitation.aip.org/content/aip/journal/jcp/89/3?ver=pdfcov
Published by the AIP Publishing

# Monte Carlo lattice simulation of amphiphilic systems in two and three dimensions

R. G. Larson
*AT&T Bell Laboratories, Murray Hill, New Jersey 07974*

(Received 29 December 1987; accepted 12 April 1988)

Microstructures such as 2D micelles (in two dimensions) and lamellar arrays, cylinders, and spheres (in three dimensions) are allowed to self-assemble via Monte Carlo simulation of an idealized lattice model for amphiphile–oil–water systems. Energies, free energies, equilibrium phase diagrams, and solution microstructures are estimated by Monte Carlo sampling of configuration space. In two dimensions (2D) at a temperature at which oil units have only a 3% solubility in the water phase, amphiphile at 20% concentration solubilizes any ratio of oil and water into a single phase and at lower concentrations produces phases with ultralow interfacial tension between them. As expected, in 3D solubilization is weaker and interfacial tensions higher than in 2D at comparable temperatures. Nevertheless, 3D systems containing the longest amphiphile (four head and four tail units) shows ordered solution structures, such as micelles at modest amphiphile concentration and periodic lamellar and cylindrical structures at high amphiphile concentration that are analogous to those of diblock polymers mixed with low molecular weight homopolymers.

## I. INTRODUCTION

Surfactant-containing solutions have unusual properties associated with the tendency of surfactant molecules to form microstructured solutions. Typical properties include the ability of modest concentrations of surfactant to *solubilize* two antagonistic liquids, such as oil and water, into a single equilibrium phase, and formation, at high surfactant concentrations, of liquid–crystalline phases. All surfactant molecules are *amphiphilic*; i.e., they contain both water-loving and oil-loving moieties. But some amphiphiles, such as small alcohol molecules, do not form the above solution structures, and are thus not considered surfactants. Both surfactant-like and alcohol-like amphiphiles are considered in the simulations presented here.

Surfactants mixed with aqueous and/or hydrocarbon components form a wide range of fascinating microstructures, including randomly dispersed and orderly packed globules and cylinders as well as flat (lamellar) or curved (vesicular) multilayers and bicontinuous structures. The prediction of equilibrium microstructure from molecular architecture and intermolecular interactions is an extremely challenging theoretical goal, towards which considerable progress is being made, through both analytic and computer-simulation approaches.

In the analytic approach, physically motivated simplifications are sought whereby one can dodge the multiple body interactions inherent in the problem. Simple *space-filling packing arguments*,[1,2] together with an estimated optimal surface area per surfactant, allow one to predict micellar and vesicular structures in dilute surfactant solutions. Thus compact objects such as spherical micelles are predicted—and indeed observed—to give to less compact objects such as cylinders and bilayers as the effective cross-sectional area of the head or water-loving component of the surfactant becomes smaller (through addition of salt to ionic surfactants, for example) relative to the effective cross-sectional area of the tail or oil-loving moiety. More detailed information has been provided through *self-consistent mean-field approximations* whereby the configuration of a test surfactant molecule (in a micelle, say) is computed in a mean field created by surrounding surfactants, which are assumed to have the same average properties as the test chain.[3,4] A class of analytic theories for *random bicontinuous microemulsions* has been spawned by the work of Talmon and Prager.[5–8] They coarse grained the molecular description away and assumed that all the surfactant resides in sheets that divide oil and water regions from each other. In these latter theories molecular properties appear only implicitly through their influence on phenomenological surface curvature and curvature-fluctuation parameters. The analytic approach as a whole suffers the drawback that the class of allowed microstructures is assumed *a priori*; one then deduces which of the assumed microstructures has the lowest free energy and therefore is the most stable of *those considered*. In addition to ignoring complex or as yet unimagined microstructures, the analytic approach is not well suited to deal with situations in which fluctuations in size or shape are large, or indeed the microstructure itself fluctuates from one topology to another.

The second general approach, that of Monte Carlo or molecular dynamics simulation, has the potential to address limitations of the analytic approach. Techniques have progressed to where they are yielding useful physical insight.[9–11] Unfortunately, however, computers are not yet fast enough to allow both accurate description of real intermolecular interactions and self-asssembly of arbitrary microstructures. Two complementary kinds of simulation are, however, now feasible. In the first kind, the microstructure is prescribed *a priori* as in the analytic approach: single globular micelles[9–11] and bilayers[10] have been studied thus far. In the second kind of simulation, accurate molecular description is not attempted—the surfactants and other molecules are endowed with only their most essential features—but *molecules are allowed to self-assemble into the microstructure they prefer.* This latter kind of simulation addresses directly the limitations of the analytic approach. The first steps of this kind have been taken in two-dimensional Monte Carlo lattices

 0021-9606/88/151642-09$02.10 

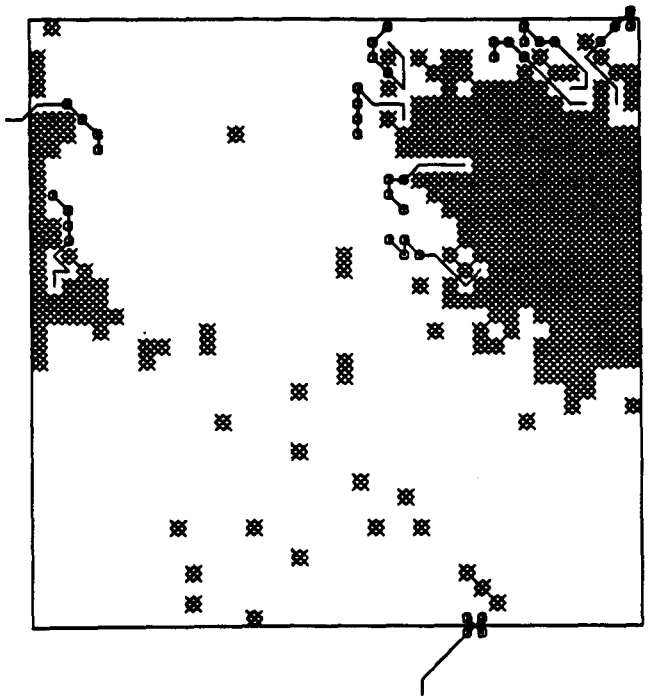

FIG. 1. Example of two-dimensional lattice model with amphiphile head units (circles), tail units (lines), oil units (shaded), and water units (blank).

studies by Larson[12] and by Care.[13] Larson's simulations showed micellar cluster formation, and allowed one to estimate equilibrium solubilization of oil and water into the micellar phase. Care has computed the average micellar cluster size as a function of temperature and of the intermolecular energy parameters.

The work presented here is an extension of Larson's earlier 2D work to longer 2D runs and to 3D lattices. In the simulation, oil and water molecules occupy single sites on the lattice and the amphiphile occupies a sequence of contiguous sites, as in Fig. 1. Here a contiguous site is either a nearest neighbor or a diagonal nearest neighbor. Each site therefore has $z = 8$ contiguous sites in 2D and $z = 26$ in 3D, where $z$ is the coordination number. The structure depicted in Fig. 1 evolved from an initially random spatial distribution of amphiphile molecules after several million attempted moves.

The highly idealized model amphiphiles considered here are crude models of surfactant molecules that are known to form interesting microstructures in solutions with water and/or oil. Although the tail units of real surfactants can be similar chemically to the oil molecules they are mixed with, the head units of real surfactants are usually similar to water molecules only in their strong polarity. The variety of possible energetic (and steric) interactions between real surfactant head groups and water is, in part, responsible for the rich diversity of behavior possible in these systems.[14,15] Although this diversity connot be described in detail by the idealized model considered here, a study of the ideal systems could perhaps form a common base to which the variety of complications occurring in real systems may be related.

The *energetics* of our ideal system actually has much more in common with mixtures of block polymer A–B in low molecular-weight homopolymers A and B than with surfactant mixtures. The statistics, and consequently the entropies, of our short-molecule systems are, however, different from those of polymers. Nevertheless, in our amphiphilic system, we will report composition-dependent transitions in microstructure from lamellar to cylindrical to spherical that are analogous to those seen in the block polymer systems.[16] To our knowledge this represents the first molecular simulation of these microstructural transitions in amphiphilic systems.

## II. MONTE CARLO TECHNIQUE

In the simulations, initially random configurations evolve toward configurations typical of equilibrium by the usual Metropolis scheme, in which many small *transitions* in molecular configuration occur sequentially. The probability that a given transition occurs is biased by the energy change resulting from the transition. For a given temperature, transitions that reduce the system energy occur with enough greater probability than those that increase it that thermal equilibrium is eventually achieved. The types of transition allowed are depicted in Fig. 2; these were chosen because they allow a relatively rapid approach to equilibrium. The usual periodic boundary conditions are used. Details of the simulation technique can be found in Ref. 12.

On the ternary oil–water–amphiphile diagram, such as Fig. 3, the location of the envelope, below which multiple phases appear at equilibrium for the lattice model, is estimated through calculation of the free energy of mixing of the three components in various ratios. Free energies are calculated by first computing canonical ensemble averages of the total system energy, this being the sum of the interaction energies of all nearest-neighbor and diagonal nearest-neighbor pairs of units. For simplicity, the interaction energy of a head unit with any other unit is assumed to be the same as

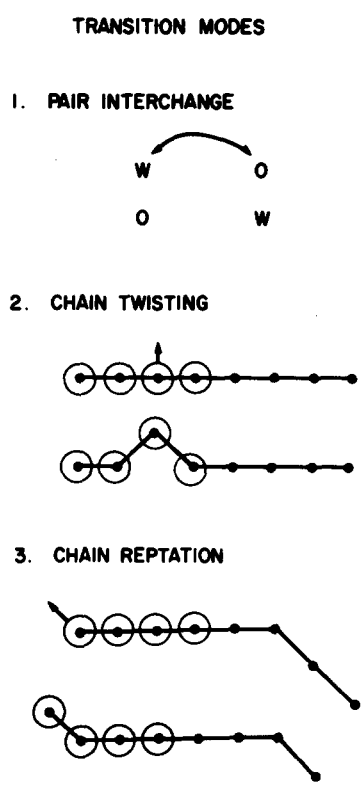


FIG. 2. The three transition modes allowed in the Monte Carlo algorithm.

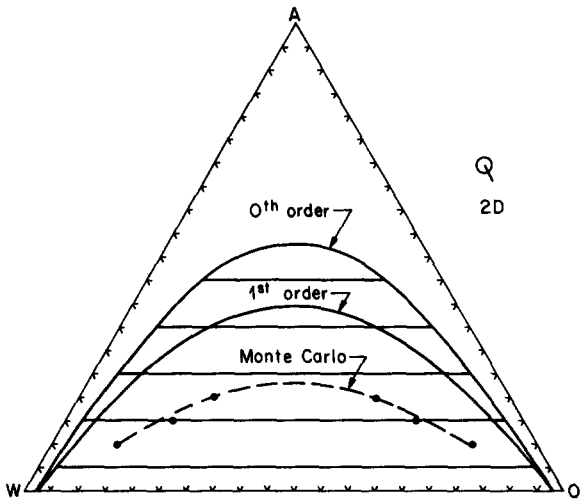


FIG. 3. Zeroth-order, first-order (quasichemical), and Monte Carlo phase diagrams for $H_1T_1$ amphiphile on the square lattice.

that of a water unit. Likewise, oil and tail units are assumed identical in their interactions with other units. Thus, the amphiphile is a string of oil (lyophilic) units and water (hydrophilic) units. There are, therefore, three types of interaction: hydrophilic–hydrophilic, hydrophilic–lyophilic, and lyophilic–lyophilic, each with its own interaction energy, $E_{HH}$, $E_{HL}$, and $E_{LL}$, respectively. The net energy of mixing is a multiple of the combination, $W \equiv E_{LH} - \frac{1}{2}E_{LL} - \frac{1}{2}E_{HH}$. Thus the ratio $w = W/kT$ is the only energetic parameter in the simulation.

The average dimensionless energy of mixing is $E = w\langle X_{HL}\rangle$, where $\langle X_{HL}\rangle$ is the ensemble average of the number of hydrophilic–lyophilic interactions. By computing this energy at a sequence of temperatures, the Helmholz free energy $F$ can be estimated from a Gibbs–Helmholz equation,

$$\frac{\partial(F/T)}{\partial(1/T)} = E. \tag{1}$$

Starting at an infinite temperature, $w = 0$, where the free energy is well approximated by an expression of Guggenheim[17] for athermal lattice mixtures, the free energy at $w = 0.5$ in 2D and $w = 0.1538$ in 3D is estimated by a trapezoidal-rule integration of Eq. (1) using average energies computed at the inverse dimensionless temperatures $w$ listed in Table I. (See Ref. 12 for details.) Test calculations with smaller steps in $w$ were carried out; these did not yield any significant departure from the free energies obtained using the $w$ values of Table I, and therefore, the steps between values of $w$ given in Table I were deemed small enough. $w = 0.1538$ on the 3D lattice is comparable to $w = 0.5$ on the 2D lattice because both correspond to a temperature that is about 60% of the critical temperature for the binary mixture of oil and water units; in both two and three dimensions, $zw = 4$.

## III. REFINED RESULTS IN TWO DIMENSIONS

### A. Free energies

In this paper, a more refined estimate of the location of the multiphase envelope than that reported in the earlier paper for the 2D systems is obtained from larger and more numerous computer runs than those of the earlier paper; see Table I. Figure 4 shows the free energy, from both the new runs and the earlier runs, of a mixture of 20% amphiphile as a function of oil concentration. For this plot the amphiphile, $H_1T_1$ contains one head unit and one tail unit. As shown in Table I, the more recent runs are 50 times longer than earlier runs, and consequently the error bars[18] of the new runs are about seven times smaller than those of the earlier runs. The greater precision of each new run and the greater number of oil concentrations sampled allow a more precise determination of the oil concentration at which the transition occurs between one and two phases at equilibrium, or between two and three phases, as discussed below.

### B. Phase behavior and interfacial free energy

Free energies and phase diagrams computed by Monte Carlo calculation are compared with the predictions of analytic lattice theories for weakly associating molecules. In the zeroth order theory, which is similar to the Flory–Huggins theory, the solution is assumed to be a random mixture of molecules. The numbers of hydrophilic–lyophilic, hydrophilic–hydrophilic, and lyophilic–lyophilic interactions are then related to each other by

$$(\tfrac{1}{2}X_{HL})/(X_{LL}\,X_{HH}) = 1. \tag{2}$$

In the first-order *quasichemical* theory, a given unit tends to attract units with which it interacts favorably; but this attraction is so weak that each *pair* of units is independent of neighboring pairs. In the quasichemical theory,

TABLE I. Number of configurations sampled in each Monte Carlo run.[a]

| $w$(2D) | Reference 12 40×40 | This work 40×40 or 100×100 lattices | $w$(3D) | This work 20×20×20 lattices |
|---|---|---|---|---|
| 0.10 | 100 000 | 5 000 000 | 0.0308 | 5 000 000 |
| 0.20 | 250 000 | 12 500 000 | 0.0615 | 12 500 000 |
| 0.30 | 250 000 | 12 500 000 | 0.0923 | 12 500 000 |
| 0.40 | 500 000 | 25 000 000 | 0.1231 | 25 000 000 |
| 0.45 | 1 000 000 | 50 000 000 | 0.1385 | 50 000 000 |
| 0.50 | 1 000 000 | 50 000 000 | 0.1538 | 50 000 000 |
| Total | 31 000 000 | 155 000 000 | | 155 000 000 |

[a] In the new work reported here, each 2D run with 155 000 000 configurations required approximately 8 h of computer time on an Alliant FX1 computer; 3D runs each took about 24 h.

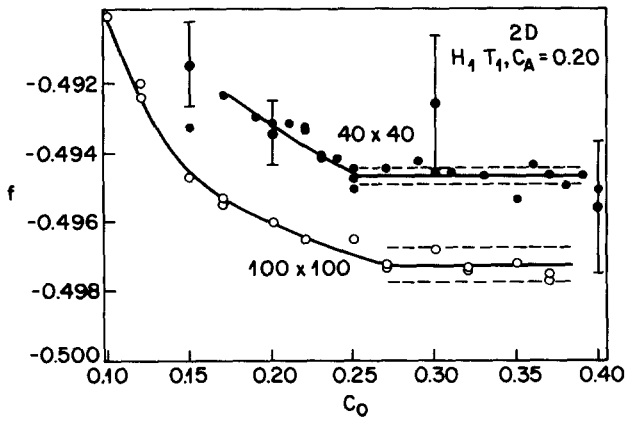


FIG. 4. Free energy $f$ vs oil concentration $C_0$ for 20% $H_1T_1$ on $40\times40$ and $100\times100$ lattices. The points with large error bars are "short runs" on $40\times40$ lattices from Ref. 12. The dashed lines are error bounds for the refined runs of this work.

$$(\tfrac{1}{2}X_{HL})/(X_{LL}\,X_{HH}) = e^{-2w}, \tag{3}$$

we shall consider only the free energies of solutions with amphiphiles containing equal numbers of head and tail units. The phase diagrams of these systems are symmetric about an oil/water ratio of unity. At low or modest amphiphile concentration, there are two possible types of behavior. The first type, depicted in Fig. 3, contains a single binodal envelope. According to the zeroth- and first-order (quasichemical) theories, the amphiphile $H_1T_1$ exhibits this type of phase behavior. For this type of phase behavior, at a fixed amphiphile concentration, the free energy per unit site $f$ plotted against oil concentration $C_0$ becomes independent of $C_0$ inside the binodal envelope, if contributions from interfacial free energy are negligible. Figure 4, for example, shows constancy of $f$ on the $40\times40$ lattice for $C_0 > 0.25$. Thus, for this first type of diagram, the location of the binodal envelope at a given amphiphile concentration can, in principle, be determined by finding the oil concentration at which $f$ becomes independent of $C_0$. The second type, shown in Fig. 5, contains a three-phase triangle bounded on each side by a two-phase region. For this type of diagram, $f$ becomes independent of $C_0$ only inside the three-phase triangle. Thus, for this latter type of diagram, the oil concentration at which $f$ becomes independent of $C_0$ determines the transition between three and two coexistent phases, again assuming that interfacial free energy is negligible. It is not possible, from plots of free energy vs oil concentration, such as Fig. 4, to distinguish between the two types of transition in the Monte Carlo simulations. The zeroth- and first-order theories suggest, however, that all amphiphiles except $H_1T_1$ have three phase coexistence triangles. In any event, the locus of oil concentrations $C_0^*$ at which the phase transition occurs, plotted against amphiphile concentration on a ternary diagram, defines a phase envelope, either a single binodal envelope for the first type of diagram, or a three phase triangle for the second type. In either of the two cases, the envelope determined in this way gives an estimate of the height of the multiphase region, and thus the solubilizing power of the amphiphile.

For mixtures that contain no amphiphile, the interfacial free energy is not negligible, as is shown in Fig. 6. Here, the free energy as a function of oil concentration is minimum at the transition between one and two equilibrium phase. If interfacial free energy were negligible, $f$ would remain constant as $C_0$ is increased beyond the point of phase separation, $C_0^*$. The increase in $f$ as $C_0$ increases beyond $C_0^* \approx 0.03$ apparently comes from the growing contribution of interfacial free energy as one progresses deeper into the two phase region. The free energy per site that must be associated with the interface reaches a value somewhat higher than 0.02 dimensionless units. For the 2D systems *with amphiphile*, the interfacial free energy is too small to be discerned even by the refined Monte Carlo calculations of Fig. 4. Since the average error in the free energy for the refined calculations is about 0.0002, we conclude that in 2D the amphiphile $H_1T_1$ in 20% concentration reduces the interfacial energy by a factor of 100 or more below that of the binary oil/water mixture!

Because of the greater refinement of the recent calculations, much smaller levels of departure of $f$ from constancy are detected than were detectable in the earlier calculations. The typical estimated error in the earlier free energy calculations for $H_1T_1$ is 0.0015; this is half the average height of the large error bars in Fig. 4. (The vertical coordinates of Fig. 4

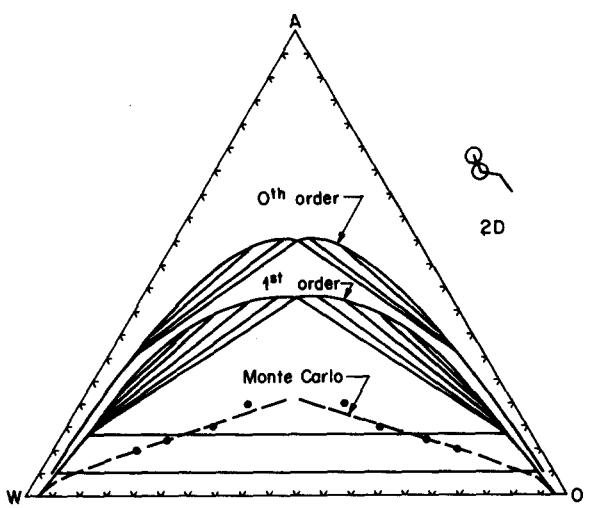


FIG. 5. Zeroth-order, first-order (quasichemical), and Monte Carlo phase diagrams for $H_2T_2$ amphiphile on the square lattice.

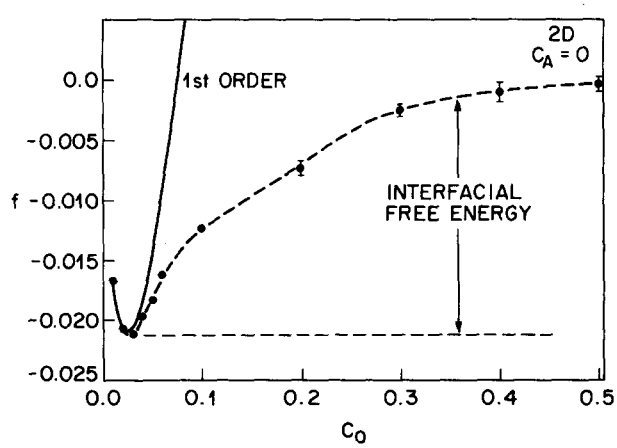


FIG. 6. Monte Carlo and first-order (quasichemical) free energies on the $40\times40$ lattice with no amphiphile.

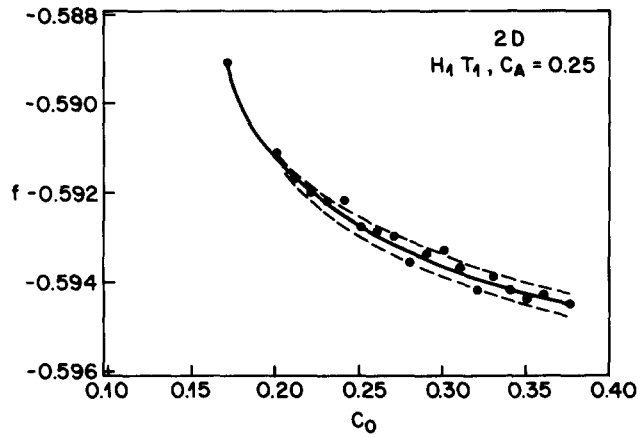


FIG. 7. Free energy vs oil concentration $C_0$ for 25% $H_1T_1$ on a 40×40 lattice. The dashed lines are error bounds. Note the absence of a region of constant $f$, indicating that this concentration of amphiphile lies above the multiphase envelope.

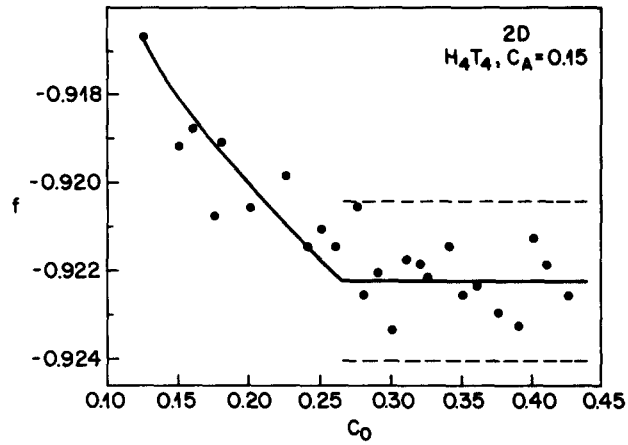


FIG. 9. Free energy $f$ vs oil concentration $C_0$ for 15% $H_4T_4$ on a 40×40 lattice.

are plotted on a highly expanded scale compared to that of comparable plots in Ref. 12.) In the refined calculations this error is reduced to 0.0002, and the height of the error band (shown by dashed lines) to 0.0004. Thus indication of a phase transition is now found at a higher value of $C_0$ than was possible in the presence of the larger errors of the earlier calculation. For each amphiphile studied here, at each amphiphile concentration $C_A$, the refined calculations therefore show a *higher* value of $C_0^*$ than was found in the earlier simulations. Further refinement could presumably further increase $C^0$.

For each amphiphile, $H_1T_1$, $H_2T_2$, and $H_4T_4$, plots of free energy vs oil concentration at several levels of amphiphile concentration were obtained. Figures 4 and 7–9 are representative examples. From each plot, $C_0^*$ was obtained; the multiphase envelopes, given by the locus of values of $C_0^*$ for each $C_A$, are shown in Figs. 3, 5, and 10. For each of the three amphiphiles, the refinement in calculation leads to a *reduction* in the estimated height of the multiphase envelope from the estimate based on the earlier calculations. Contrary to the indications from the earlier crude calculations of Ref. 12, the height of the envelope decreases as the amphiphile length increases.

### C. Lattice size effect

The refinement of the recent calculations also allows discernment of a lattice size effect not evident in the earlier calculations. Figure 4 shows that free energies of 100×100 systems are *lower* than those for 40×40 systems. The location of $C_0^*$ estimated from the 100×100 lattice is perhaps slightly larger than that estimated for the 40×40 lattice. The smaller system, however, has the advantage that for a given total number of Monte Carlo steps, it will equilibrate more thoroughly than the larger system (because each unit on the smaller lattice has more opportunities to move). For the runs of 155 million steps, each unit on a 40×40 lattice has 100 000 chances to move. The phase diagrams shown in Figs. 3, 5, and 10 were all obtained from 40×40 lattices.

## IV. THREE DIMENSIONAL CALCULATIONS

### A. Phase behavior and interfacial free energy

The calculations of phase behavior in 3D were carried out on 20×20×20 lattices. As with the 2D systems, free energies were obtained by integrating the average energies obtained at a sequence of inverse temperatures $w$; the values

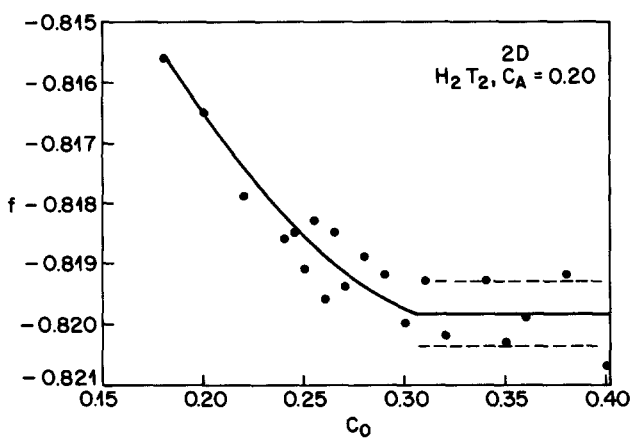


FIG. 8. Free energy $f$ vs oil concentration $C_0$ for 20% $H_2T_2$ on a 40×40 lattice. The dashed lines are error bounds.

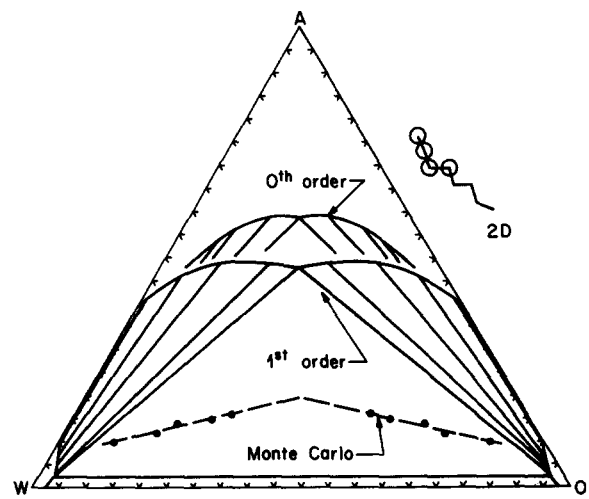


FIG. 10. Zeroth-order, first-order (quasichemical), and Monte Carlo phase diagrams for $H_4T_4$ amphiphile on the square lattice.

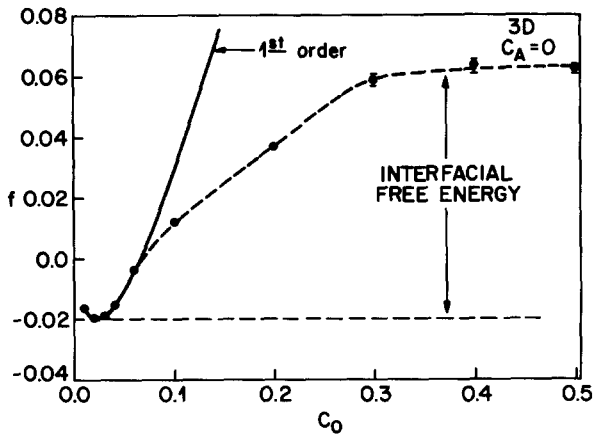


FIG. 11. Monte Carlo and first-order (quasichemical) free energies on the 20×20×20 lattice with no amphiphile.

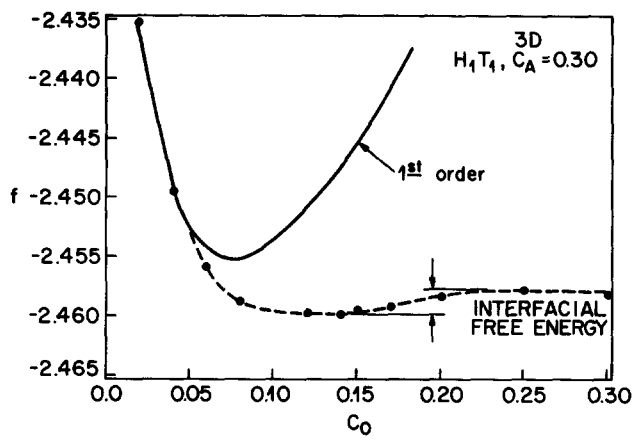


FIG. 13. Free energy $f$ vs oil concentration $C_0$ for 30% $H_1T_1$ on the 20×20×20 lattice.

of $w$ used and the number of Monte Carlo attempts at each value of $w$ are given in Table I. Figure 11 shows $f$ vs $C_0$ in the absence of amphiphile for the cubic lattice. As happens in 2D, there is a significant contribution from interfacial free energy. Figure 12 shows that for 20% $H_1T_1$, the interfacial free energy is significant in 3D, whereas we noted that it is too small to be discerned in the 2D calculations. In 3D, $H_1T_1$ at a concentration of 20% reduces the interfacial energy by a factor of about 8 below that of pure oil and water; in 2D the reduction is 100-fold or greater. At a concentration of 30% $H_1T_2$ in 3D, the amphiphile reduces the interfacial free energy 40-fold; see Fig. 13.

Note in Figs. 12 and 13 that the free energies of 3D systems containing $H_1T_1$ depart only slightly (0.2% or less) from the quasichemical predictions in the single phase region. For the 2D systems, the departure is larger; the predictions of the quasichemical theory, which are off-scale in Figs. 4 and 7–9, are approximately 2% higher (i.e., less negative) than the Monte Carlo predictions for $H_1T_1$. For $H_4T_4$ in 2D, the difference is roughly 7% in 2D and 2% in 3D. In 3D the phase envelope for $H_1T_1$ is close to the location predicted by quasichemical theory, Fig. 14. This improved agreement with quasichemical theory is not surprising since both increased dimensionality and increased coordination number generally improve the predictions of mean-field theories, such as the quasichemical theory. In sum, in 3D at the inverse temperature $w = 0.1538$, the amphiphile $H_1T_1$ neither produces orders-of-magnitude reduction in interfacial energy (except near the critical points) nor creates solution structure that is greatly different from the weak binary association assumed by the quasichemical theory. Thus in 3D, $H_1T_1$ acts more like an alcohol than a surfactant.

The relatively long amphiphile $H_4T_4$ at a concentration of 20%, however, reduces the interfacial free energy below the threshold of measurability; see Fig. 15. Considering the estimated magnitude of the error in the calculation of free energy for this system, this represents a reduction of factor of 12 or more in the interfacial free energy below that of the pure oil/water mixture. In addition, the free energies and phase behavior of $H_4T_4$ depart significantly from the quasichemical theory.

Note in Fig. 15 that the typical error bar calculated for 20% $H_4T_4$ in 3D is considerably larger than the scatter in the Monte Carlo free energies. As described in detail in Ref. 12, the error is calculated by comparing the energies averaged over the first half of the Monte Carlo run with energies averaged over the second half. This method yields an accurate

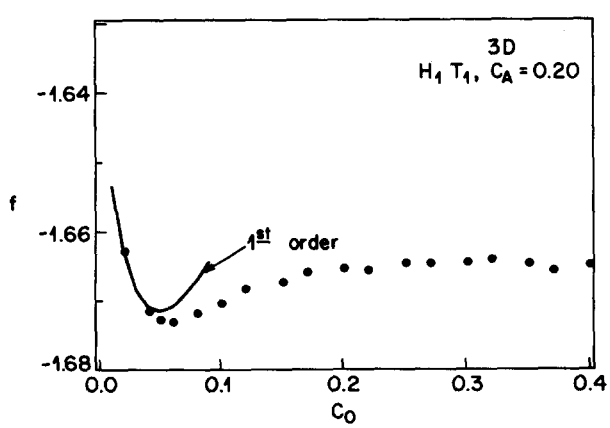


FIG. 12. Free energy $f$ vs oil concentration $C_0$ for 20% $H_1T_1$ on the 20×20×20 lattice.

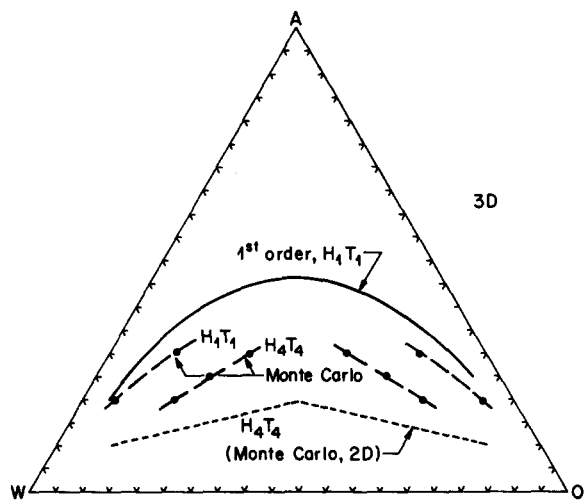


FIG. 14. Phase diagrams for $H_1T_1$ and $H_4T_4$ amphiphiles on the cubic lattice compared with results for $H_1T_1$ on the square lattice.

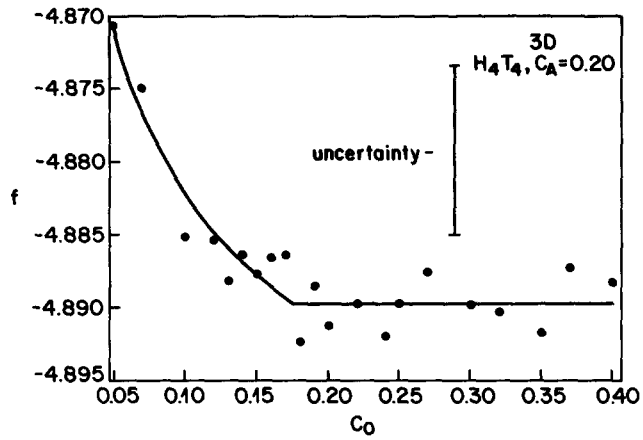


FIG. 15. Free energy $f$ vs oil concentration $C_0$ for 20% $H_4T_4$ on the $20\times20\times20$ lattice.

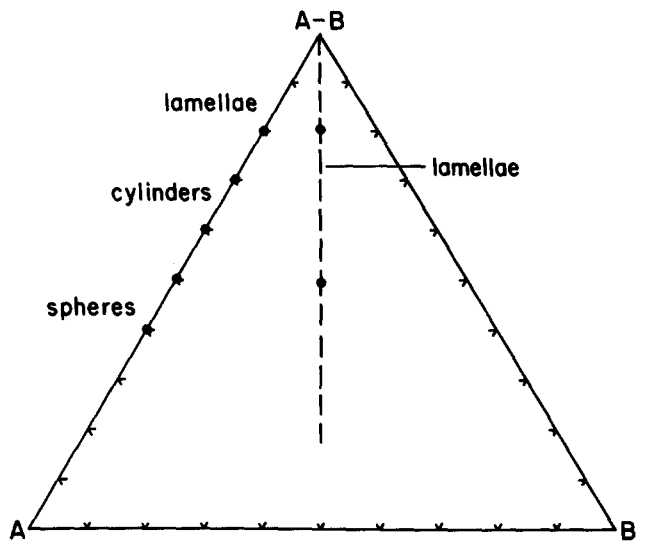


FIG. 16. Three component triangular composition diagram with volume fractions amphiphile(A–B), oil(A), and water(B).

estimate of the error only if, after the start of the simulation, the system rapidly reaches a configuration typical of equilibrium and then fluctuates without systematic drift. For $H_4T_4$ systems in 3D, however, we find that the energy averaged over the first half of the run is usually higher than that averaged over the second half, showing that these averages are those of a system still drifting toward equilibrium. Our experience with short runs in 2D systems (such as those in Ref. 12) lead us to believe that the phase envelope for $H_4T_4$ in 3D could be considerably lower than the estimate shown in Fig. 14.

### B. Microstructure at high amphiphile concentrations

In the simulations, oil, water, and amphiphiles are initially randomly dispersed on the lattice, and the system is gradually "cooled" from infinite temperature, that is $w = 0$, to the temperature of interest, $w = 4/z = 0.1538$, as discussed in Sec. II. The effect of lattice size on microstructure is investigated by performing runs on $10\times10\times10$, $15\times15\times15$, and $20\times20\times20$ lattices, with the cooling regime given in Table II.

The compositions examined in this portion of the study are marked on the three-component triangle in Fig. 16. These compositions can be grouped in two progressions. In progression I, which runs down the center of the triangle, the amphiphile concentration is progressively lowered from 0.8 to 0.5, holding the oil/water ratio fixed at unity. In progression II, which runs down the side of the triangle, the water concentration is held fixed at zero. In experimental mixtures of diblock polymers, A–B, mixed with low molecular weight homopolymers A and B, progression I produces only lamellar morphologies. Progression II produces transitions from lamellar morphologies at high concentrations of block polymer to cylinders to spheres as the block polymer concentration is lowered, according to Hashimoto.[16]

Figure 17(a) shows the locations of head units on a typical slice through a $10\times10\times10$ cubic lattice, for the highest concentration of amphiphile in progression I. The slice is parallel to a face of the cube. The square bounded by dashed lines contains the simulated region; the rest of the figure is filled by periodic images. A lamellar structure is evident with a repeat spacing equal to ten lattice sites, which is the length of an edge of the lattice. Apparently, because this lamellar spacing is incommensurate with the edge of a $15\times15\times15$ lattice, the lamellae orient along the diagonal of the $15\times15\times15$ lattice; see Fig. 17(b). On a $20\times20\times20$ lattice, Fig. 17(c), the lamellae orient at an angle intermediate to that of a parallel and a diagonal orientation. Concentrations of amphiphile as low as 50% in progression I were investigated; lamellar morphologies were always obtained.

Figure 18 shows two slices through a $15\times15\times15$ lattice with 80% amphiphile in progression II, that is, with no water. Most of the slices have the morphology of Fig. 18(a), that is lamellae. However, in a thin slab of the cubic lattice,

TABLE II. Number of configurations in runs at high amphiphile concentrations.

| $w$ | $10\times10\times10$ or $15\times15\times15$ lattices | $20\times20\times20$ lattices |
|---|---|---|
| 0.0308 | 5 000 000 | 20 000 000 |
| 0.0615 | 12 500 000 | 50 000 000 |
| 0.0923 | 12 500 000 | 50 000 000 |
| 0.1231 | 25 000 000 | 100 000 000 |
| 0.1385 | 50 000 000 | 200 000 000 |
| 0.1538 | 50 000 000 | 200 000 000 |
| Total | 155 000 000 | 620 000 000 |

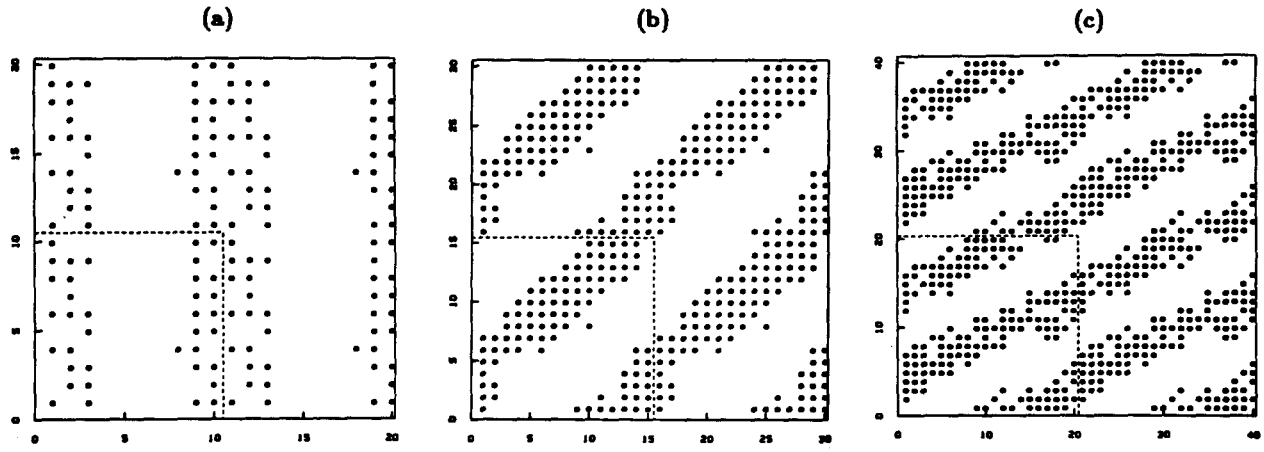


FIG. 17. Typical slices through cubic lattices with 80% amphiphile, 10% oil, and 10% water. Only the head units are shown. (a) $10\times10\times10$; (b) $15\times15\times15$; (c) $20\times20\times20$.

the lamellae are ripped, as Fig. 18(b) shows. When the amphiphile concentration is lowered to 70%, Fig. 19(a), most of the slices show the discrete patches of head groups. The patches on each slice are connected to each other, forming pillar-like or cylindrical structures that connect to a thin slab with lamellar morphology, depicted in Fig. 19(b). For amphiphile concentrations of 60% and 50%, the morphology is purely cylindrical, with no interleaving of lamellae. This progression is consistent with a phase diagram in which lamellae prevail above about 85% amphiphile, and cylinders below about 65%, with coexistence of cylindrical and lamellar phases between about 65% and 85% amphiphile. For simulations with amphiphile concentrations of 40% and 30%, the head groups cluster in globular or spherical morphologies. Thus the progression, lamellae→cylinders→spheres, observed in the block polymer system also appears in this model amphiphile system.

Combining the phase diagram obtained from simulations at low amphiphile concentration with the lamellar morphology found in progression I and the suggestion of coexistence of first lamellae and cylinders and then cylinders and spheres along progression II, we construct an overall phase diagram, Fig. 20. This speculative diagram is perhaps the simplest one that agrees with the above tentative findings, and is symmetric about an oil/water ratio of unity. The development of more powerful computers should make possible the refinement or correction of the suggested phase diagram.

## V. CONCLUDING REMARKS

Our Monte Carlo lattice model shows that computer power is reaching the level necessary to investigate by simulation the influence of simple molecular properties, such as length of head and tail groups and the strength of nearest-

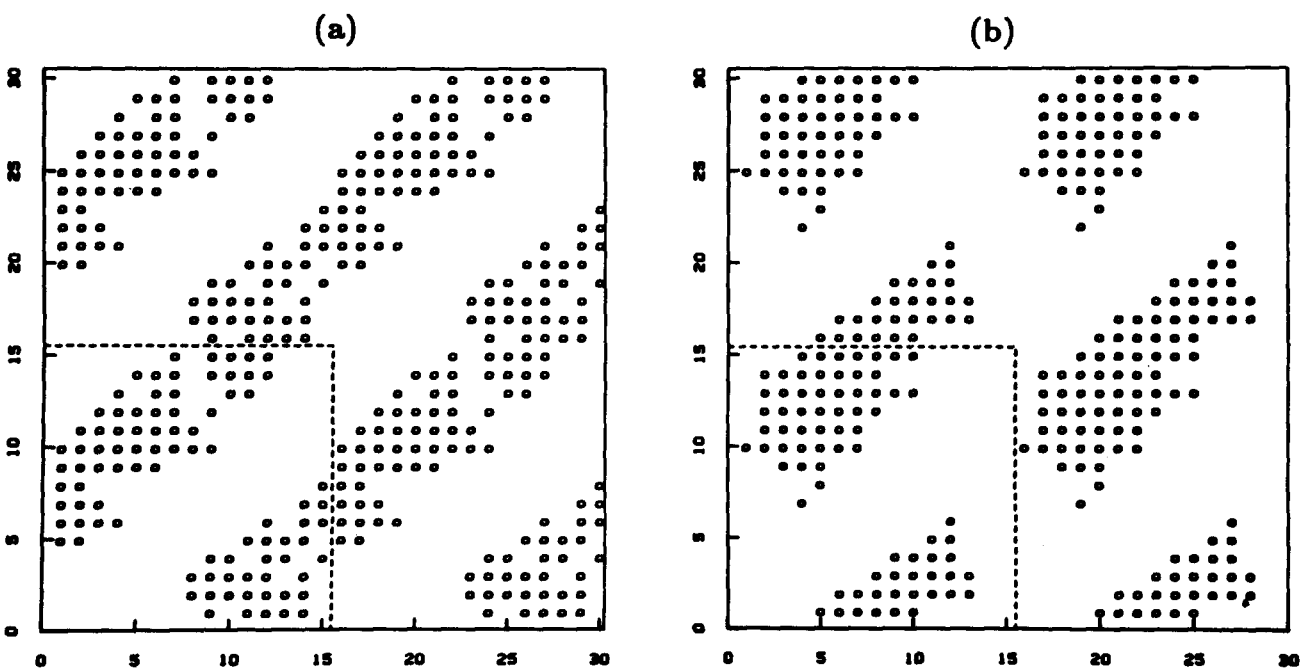


FIG. 18. Slices through a $15\times15\times15$ lattice with 80% amphiphile, 20% oil, and 0% water. Most of the slices have the morphology of (a).

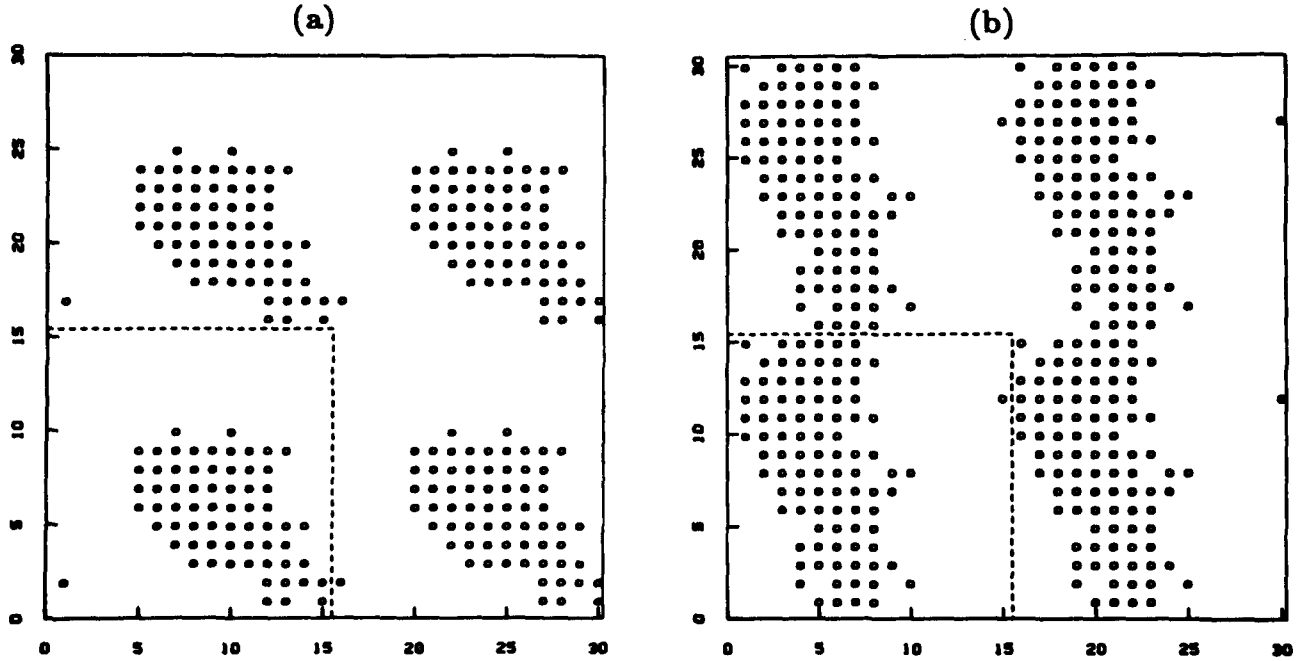


FIG. 19. Slices through a 15×15×15 lattice with 70% amphiphile, 30% oil, and 0% water. Most of the slices have the morphology of (a).

neighbor interactions, on the three-dimensional equilibrium microstructure and phase behavior of surfactant systems. The lattice model is rudimentary, but contains the essential ingredients: the amphiphile can be made long enough and the interactions made strong enough to force microseparation of hydrophilic and lipophilic moieties. Thus the longest amphiphile considered here produces substantial solubilization (even in three dimensions) low interfacial tensions, and lamellar, cylindrical, and spherical microstructures. In a future communication, we shall report the appearance of periodic *bicontinuous structures* in systems for which the heads and tails are of unequal length. Most importantly, these microstructures *self-assemble*, and thus we show the feasibility of calculating the true equilibrium microstructure without restricting in advance the allowed possibilities. Though the molecular architectures (of surfactant, oil, and water) and the intermolecular interactions assumed in the model are clearly too simple to describe real surfactant systems in any detail, the richness of the observed bahavior will make these kinds of simulations interesting ones with which to test analytic theories. After all, if analytic theories of surfactant microstructure and phase behavior are to address the complexities of real systems, they ought *a fortiori* to be able to handle the much simpler (but still rich) behavior of the lattice model presented here.

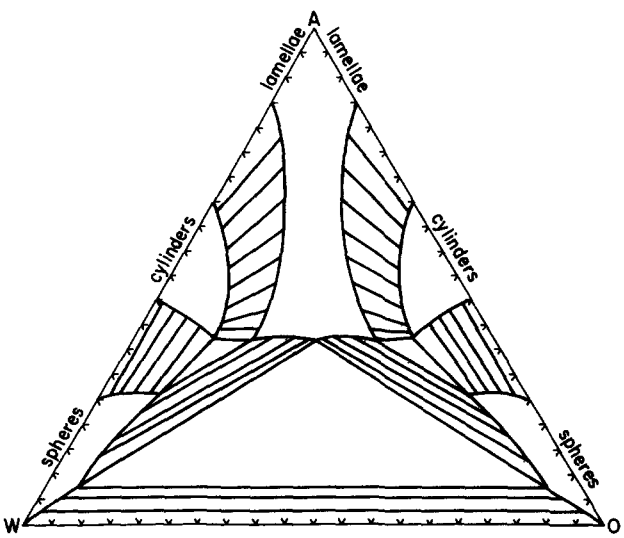


FIG. 20 Speculated form of phase diagram for $H_4T_4$ on the cubic lattice.

## ACKNOWLEDGMENTS

I gratefully acknowledge the impetus provided to this work through discussions with Ted Davis, Skip Scriven, Stephen Prager, Wilmer Miller, and members of the low-tension research group at the University of Minnesota.

[1]J. N. Israelachvili, D. J. Mitchell, and B. W. Ninham, J. Chem. Soc. Faraday Trans. 2 **72**, 1525 (1976).
[2]D. F. Evans, D. J. Mitchell, and B. W. Ninham, J. Phys. Chem. **90**, 2817 (1986).
[3]A. Ben-Shaul and W. M. Gelbart, Annu. Rev. Phys. Chem. **36**, 179 (1985).
[4]D. W. R. Gruen, J. Phys. Chem. **89**, 146 (1985).
[5]Y. Talmon and S. Prager, J. Chem. Phys. **69**, 2984 (1978).
[6]P. G. de Gennes and C. Taupin, J. Phys. Chem. **86**, 2294 (1982).
[7]B. Widom, J. Chem. Phys. **84**, 6943 (1986).
[8]D. A. Huse and S. Leibler, J. Phys. (Paris) (in press).
[9]B. Owenson and L. Pratt, J. Phys. Chem. **88**, 2905 (1984).
[10]P. van der Ploeg and H. J. C. Berendsen, Mol. Phys. **49**, 233 (1983).
[11]J. M. Haile and J. P. O'Connell, J. Phys. Chem. **88**, 6363 (1984).
[12]R. G. Larson, L. E. Scriven, and H. T. Davis, J. Chem. Phys. **83**, 2411 (1985).
[13]C. M. Care, J. Chem. Soc. Faraday Trans. 1 **83**, 2905 (1987).
[14]R. G. Laughlin, in *Advances in Liquid Crystals* (Academic, New York 1978).
[15]L. E. Scriven, in *Micellization, Solubilization, and Microemulsions*, edited by K. L. Mittal (Plenum, New York 1977).
[16]T. Hashimoto, talk given at AT&T Bell Laboratories, Murray Hill, March 1987.
[17]E. A. Guggenheim, Proc. R. Soc. London Ser. A **183**, 213 (1944).
[18]The method of estimating the error bar is described in Ref. 12.